J. Chem. Sci. (2020) 132:81
https://doi.org/10.1007/s12039-020-01793-2
© Indian Academy of Sciences

REGULAR ARTICLE

DFT calculations, Hirshfeld surface analysis and docking studies of 3-anisaldehyde thiosemicarbazone

MRIDULA GUIN[a,*], SONIA KHANNA[a], S BEGAM ELAVARASI[b] and PARATPAR SARKAR[a]

[a]Department of Chemistry and Biochemistry, School of Basic Sciences and Research, Sharda University, Greater Noida, India
[b]Department of Physics, Anna University, Chennai 600025, India
E-mail: mridula.guin@sharda.ac.in

MS received 10 December 2019; revised 20 March 2020; accepted 1 April 2020

Abstract. We report herein the synthesis, quantum chemical electronic structure, Hirshfeld surface and molecular docking studies of 3-anisaldehyde thiosemicarbazone (**I**). The compound has been characterized by NMR (^{1}H, ^{13}C) and IR spectroscopy. Hirshfeld surface analysis has been performed to understand the intermolecular interactions. The quantum chemical calculations show good consistency between the predicted and experimental parameters. Molecular docking studies of **I** with two different cancer target enzymes exhibit higher binding energy than its ortho substituted analogue.

Keywords. Thiosemicarbazone; 3-anisaldehyde; FT-IR; DFT; Hirshfeld surface; NMR; molecular docking.

1. Introduction

Thiosemicarbazones are important class of compounds consisting of N, S, donor atoms and have been investigated extensively with different metals.[1–3] They are prepared by the condensation of primary amines with carbonyl compounds and have received a thrust of interest because of their versatile bonding and biological activities related to the antitumor, antiviral, antitubercular, antibacterial, antihypertensive and antimalarial properties.[3] They also exhibit various interesting properties which are utilized in many analytical applications.[4,5]

Thiosemicarbazone metal compounds of iron and copper are extensively investigated for their antiproliferative activity.[6,7] Research in the area of treatment of cancer has created a considerable interest among researchers and has rapidly increased in the last few decades.[8,9] The soft donor atoms (N and S) in thiosemicarbazone ligand have the ability to form a chelate compound with suitable metals resulting a potential anticancer drug. A large number of thiosemicarbazone derivatives have been studied widely for their anticancer activities exhibiting interesting results.[10,11] The design and discovery of anticancer drugs are associated with huge failure rate in terms of toxicology and safety issues.[12–14] Theoretical methods are developed to identify the lead compounds having drug like properties. Molecular docking method is a powerful technique used by the scientists and researchers worldwide to identify the molecule in a binding site from energy and stereo chemical consideration. Identifying novel, selective anticancer moiety with a computational approach has gained much popularity in recent years.

In this article, we report the synthesis and structure of 3-anisaldehyde thiosemicarbazone (**I**) along with its spectroscopic characterization using IR and NMR (^{1}H, ^{13}C) analysis. Close intermolecular interactions in this compound were investigated by Hirshfeld surface analysis. The electronic structure of **I** has been investigated computationally by *ab initio* and density functional theory (DFT) calculations. Further, few QSAR properties are also calculated from DFT calculation. Molecular docking study has been performed to understand the binding affinity of **I** with

*For correspondence

Electronic supplementary material: The online version of this article (https://doi.org/10.1007/s12039-020-01793-2) contains supplementary material, which is available to authorized users.

Published online: 03 July 2020

topoisomerase III beta domain and Human Thioredoxin Reductase (TrxR)–Thioredoxin (Trx) enzymes. The former enzyme is essential for removal of super coiling of DNA and is considered as a good option for anticancer target[15] and the latter is an essential component of the TrxR–Trx system which plays a pivotal role in regulating multiple cellular redox signaling pathways. In recent years TrxR/Trx complex has been increasingly recognized as an important modulator of tumor development, and hence targeting this complex is a promising strategy for cancer treatment.[16] This study may help to understand the inhibitory potential behavior of **I** and provide significant implications for the development of new anticancer drugs.

2. Experimental

2.1 *Material and techniques*

^{1}H and ^{13}C NMR spectra were recorded on a JEOL-AL-400 spectrometer operating at 400 MHz. The IR spectrum was recorded on an Agilent FT-IR spectrometer.

2.2 *Preparation of 3-anisaldehyde thiosemicarbazone*

Thiosemicarbazide and 3-anisaldehyde were procured from Sigma Aldrich and used without any further purification. All other reagents and solvents were purchased from commercial sources and were of analytical grade. 3-Anisaldehyde thiosemicarbazone, (**I**), was prepared by literature method[17] with slight modification. It was prepared by refluxing a mixture of 3-anisaldehyde (2.7 mL, 0.01 mM) and thiosemicarbazide (2.008 g, 0.01 mM) in a mixture of methanol (30 mL) and water (10 mL) as the solvent medium in presence of glacial acetic acid (2–3 mL). The reaction in absolute methanol as solvent did not result in desired product. But use of methanol+water in 3:1 ratio resulted the formation of **I**. The reaction mixture was refluxed for about 3–4 h, resulting in a yellow colored solution, which was kept undisturbed. The next day, a crystalline yellow product was obtained (Scheme 1). It was recrystallized using MeOH-CH_3CN and further studied using X-ray crystallography [The cif file deposited in CCDC is assigned the number 1553591. Details of crystallographic data are included in supporting information (Table S1, Figures S1 and S2)].

m.p.: 159 °C, Yield 81%; IR (cm^{-1}): υ(N-H_2) 3394, 3278; υ(-N-H) 3153; υ(C=N) + υ(C=C) + δ (NH_2) 1591, 1533, 1468; υ (C=S) 833, 920 cm^{-1}.

^{1}H (DMSO-d_6, ppm): 11.43 (s, H); 8.00, 8.05 (d. 2H); 6.92–7.29 (m, 4H); 3.78 (s, 1H).

^{13}C (DMSO-d_6, ppm): 177.95 ppm (s, C=S), 55.30 (s, OCH_3), 110.92–142.18 (m, Ph-C), 159.57 (s, C-N)

^{1}H and ^{13}C NMR chemical shifts are in the expected range and confirms the formation of (**I**).

2.3 *Computational details*

Quantum chemical calculations using Hartree-Fock (HF) and Møller-Plesset perturbation theory of second order (MP2) were implemented using GAUSSIAN 16 program package.[18] The density functional theory (DFT) calculations were also performed for rigorous, comparative analysis of better description of experimental data for the studied compound. The DFT methods with hybrid functional are known to provide excellent compromise between accuracy and computational efficiency. For DFT calculation, the geometry optimization was carried out by CAM (Coulomb attenuated Method)-B3LYP functional,[19] which combines the hybrid qualities of B3LYP and the long range correction in order to provide high accuracy results. To compare the results, calculation using B3LYP functional was also performed. For both *ab initio* and DFT calculations, the split valence basis set 6-311++G(d,p) was chosen as the addition of polarization and diffuse functions improve the accuracy of the calculated results. The only exception is MP2 calculation which was performed using 6-311+G(d) basis set because of our limited computational resources. The initial geometry was taken from a single crystal X-ray data (CCDC 1553591) and subjected to optimization. Further, vibrational frequency calculation was performed to get IR frequencies and also to confirm the structure as true energy minima as revealed by the absence of imaginary frequencies. Moreover, some electronic properties such as energy of highest occupied molecular orbital (E_{HOMO}) and lowest unoccupied molecular orbital (E_{LUMO}), energy gap between HOMO and LUMO (E_{gap}), hardness (η), softness (σ) were calculated using Koopman's theorem.[20] Partial atomic charges were calculated using CHELPG scheme by Breneman and Wiberg.[21] This method is known to be more realistic and superior than Mulliken population analysis in terms of basis set invariability.

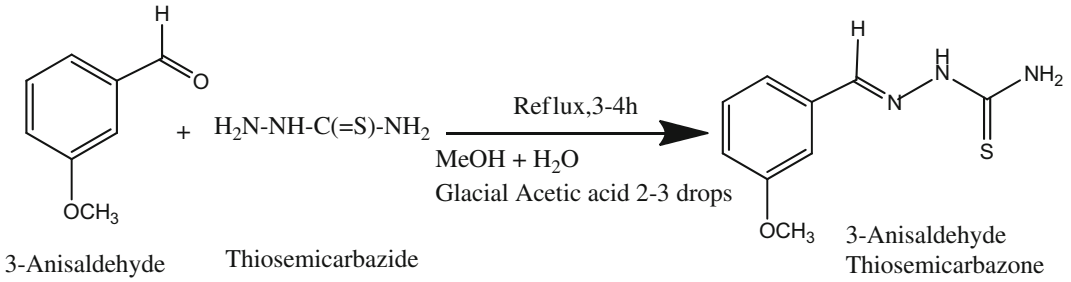

Scheme 1. Preparation of 3-anisaldehyde thiosemicarbazone (I).

2.4 *Hirshfeld surface studies*

The program Crystal Explorer 17.5,[22] was used to perform Hirshfeld surface analysis to gain additional insight and to quantify the intermolecular interactions of the molecular crystal. The calculation was performed using the cif file (CCDC 1553591) of the crystal synthesized. Hirshfeld surface analysis[23] is an effective tool for understanding intermolecular interactions and packing modes in molecular crystals. The electrostatic potential surfaces are plotted with red region which is a negative electrostatic potential (hydrogen acceptors) and blue region which is a positive electrostatic potential (hydrogen donor). The normalized contact distance d_{norm} which is related to *d*e (distance from the point to the nearest nucleus external to the surface) and *d*i (distance to the nearest nucleus internal to the surface) and the van der Waals (vdW) radii of the atom, given by equation (1), enables identification of the regions of particular importance in terms of intermolecular interactions:[24, 25]

$$d_{norm} = (d_i - r_i^{vdw})/r_i^{vdw} + (d_e - r_e^{vdw})/r_e^{vdw} \quad (1)$$

The d_{norm} values are mapped onto the Hirshfeld surface using a red–blue–white colour scheme: red regions correspond to closer contacts with negative d_{norm} value, the blue regions correspond to longer contacts with positive d_{norm} value and the white regions are those where the distance of contacts is exactly the van der Waal's separation and with a d_{norm} value of zero. Another two colour coded properties e.g. shape index and curvedness which are based on the local curvature were also mapped. The shape index is extremely sensitive to the change in surface shape. The curvedness is a measure of the shape of the surface area of the molecule. Further 2D fingerprint (FP) plot with combination of *d*e and *d*i provides summary of intermolecular contacts in the crystal. The breakdown of FP into specific atom…atom contacts in a crystal provides the types of intermolecular contacts experienced by the molecule quantitatively.

2.5 *Molecular docking study*

Patchdock server-Bioinfo 3D, a molecular docking algorithm[26] was used to carry molecular docking calculations of the synthesized compound, **I**. The ortho substituted compound 2-anisaldehyde thiosemicarbazone (**II**) has also been studied computationally to understand the effect of position of the methoxy group on binding energy with the amino acid on the active site of the enzymes Topoisomerase III beta domain (PDB id 5GVC) and Human thioredoxin reductase (PDB id 3QFA). Both the enzymes, 5GVC and 3QFA were downloaded from Protein Data Bank as PDB files. 5GVC was chosen with a resolution of 2.44 Å, R-Value free of 0.229 and R-Value work of 0.182 (https://www.rcsb.org/structure/5GVC), https://doi.org/10.2210/pdb5gvc/pdb. 3QFA was chosen with a resolution of 2.200 Å, R-Value free of 0.283 and R-Value work of 0.237 (https://www.rcsb.org/structure/3QFA), https://doi.org/10.2210/pdb3qfa/pdb. Water molecules attached to these enzymes were removed so that they do not cause any interference during the docking study. The structure of the synthesized compound **I** was drawn and cleaned using ChemSketch software and a mol file was generated which was then converted into PDB format using a smile translator. The PDB file of synthesized compound **I** was given a default PDB id of tclcactvs000-RiBvGy. For comparative study, compound (**II**) was prepared using the previously stated method and given a default PDB ligand id: tclcactvs0007SdCY. Both these compounds were then docked into the active site of two different enzymes 5GVC and 3QFA one by one. The docking was done at root mean square deviation (RMSD) of atomic position value of 4 as the standard value. The result of enzyme–compound interaction was then viewed using molegro molecular viewer. The viewing results of the docked molecules (enzyme–compound) were saved in as MVDML Format. Docking results from Patchdock produce 20 best enzyme–compound interactions in different positions.

Table 1. Selected bond lengths from calculations using 6-311++G(d,p) basis set [* for MP2 the basis set is 6-311+G(d)] and by X-ray crystallography for the compound **I**.

Bond distances (Å)						
Atom	Atom	Exp (X-ray)	(MP2)*	HF	CAM-B3LYP	B3LYP
S1	C9	1.690(17)	1.654	1.681	1.667	1.675
O2	C15	1.371(2)	1.363	1.344	1.357	1.363
O2	C22	1.422(2)	1.422	1.401	1.414	1.422
N5	N3	1.375(2)	1.357	1.355	1.353	1.355
N6	C9	1.346(2)	1.354	1.328	1.340	1.346
N5	C10	1.274(2)	1.296	1.254	1.273	1.283
N3	C9	1.314(2)	1.379	1.346	1.365	1.372
C10	C12	1.463(2)	1.462	1.475	1.464	1.462
C12	C13	1.389(2)	1.400	1.379	1.387	1.396
C12	C20	1.401(2)	1.410	1.398	1.400	1.407
C13	C15	1.389(2)	1.403	1.395	1.394	1.399
C15	C16	1.376(3)	1.402	1.382	1.389	1.396
C16	C18	1.400(3)	1.406	1.395	1.395	1.400
C18	C20	1.371(3)	1.391	1.373	1.379	1.384

Fire dock was used to filter and refine the top 10 docking results based on global energy (binding energy of the solution), attractive and repulsive van der Waals energy, atomic contact energy, geometric shape complementarity score and approximate interface area.

3. Results and Discussion

3.1 *Spectroscopic studies*

The infrared spectrum was taken in 4000–600 cm^{-1} region [see Figure S3]. Two bands between 3393 cm^{-1} and 3152 cm^{-1} represent stretching frequencies of the two N-H groups. A band at 1591 (C=N) and 833 cm^{-1}(C=S) indicates the formation of the compound. The bands are similar to the reported values with minor shifts in wavenumbers.[27,28] ^{1}H NMR spectra were recorded in DMSO-d_6 [Figure S4]. Prominent peaks were observed at 8.00 ppm and 11.43 ppm which are assigned to NH2 and NH protons respectively. The higher value of NH signal as compared to reported values[3] may be attributed to intermolecular hydrogen bonding. A signal at 3.78 ppm (due to –OCH_3) and 6.92–7.29 ppm (C-Ph) was similar to reported values in substituted anisaldehyde thiosemicarbazone.[27–29]

In ^{13}C NMR spectrum [Figure S5] the observed peaks at 178 ppm (C=S), 159.6 ppm (C=N) and 55.29 ppm (OCH_3) confirmed the formation of the compound. Signals for aromatic carbon atoms were observed in the range 111–143 ppm.

3.2 *Theoretical calculations*

The geometry of the compound **I** is optimized using four different quantum chemical levels (CAM-B3LYP, B3LYP, HF and MP2) and the optimized coordinates are listed in Table S2 to Table S5 respectively. The calculated bond distances and bond angles are presented in Table 1 and Table 2 respectively with the corresponding crystallographic data (from CCDC 1553591) for straightforward comparison. It is observed that the computed results are in agreement with the experimental data (for atomic labeling see Figure 1). Further, the results also match well with the reported crystallographic data.[17] The calculated geometrical parameters for both the DFT methods are pretty close. However, a tight comparison between the results of B3LYP and CAM-B3LYP indicates the latter to be slightly more accurate. It is observed that the bond lengths and bond angles calculated using CAM-B3LYP method are closer to the experimental value, while HF results are deviated considerably from it. This is due to the negligence of electron correlation in HF method which produces inaccurate results. The results clearly suggest CAM-B3LYP method as adequate method for describing the structure of **I** as most of the predicted parameters match well with experimentally obtained parameters. Although there are certain discrepancies which can be understood as the experimental data is for the compound in solid state whereas the calculated data corresponds for the gas phase. The optimized geometry at CAM-B3LYP method is shown in Figure 1 with atomic labeling. The calculated IR vibrational frequencies are listed in Table S6. The results indicate that for both DFT methods and MP2 method the frequencies

Table 2. Selected bond angles from calculations using 6-311++G(d,p) basis set [* for MP2 the basis set is 6-311+G(d)] and by X-ray crystallography for the compound **I**.

Bond angles (°)							
Atom	Atom	Atom	Exp	MP2	HF	CAM-B3LYP	B3LYP
C15	O2	C22	117.38(16)	116.97	119.97	118.48	118.60
C9	N3	N5	119.36(14)	121.04	121.89	121.78	122.01
C10	N5	N3	116.67(14)	116.58	117.55	117.65	117.68
N3	C9	S1	119.07(12)	120.21	120.08	120.26	120.17
N6	C9	S1	123.66(13)	125.31	123.45	124.59	124.71
N6	C9	N3	117.25(15)	114.48	116.46	115.14	115.11
N5	C10	C12	120.50(15)	121.40	122.67	122.57	122.71
C13	C12	C10	118.69(15)	118.39	117.99	118.26	118.23
C13	C12	C20	119.64(16)	119.72	119.85	119.62	119.38
C20	C12	C10	121.66(15)	121.87	122.14	122.12	122.39
C12	C13	C15	120.35(16)	120.64	120.74	120.67	120.78
O2	C15	C13	115.13(15)	115.27	115.54	115.62	115.53
O2	C15	C16	124.42(16)	124.95	124.92	124.61	124.71
C16	C15	C13	120.46(16)	119.78	119.53	119.77	119.76
C15	C16	C18	118.75(17)	119.16	119.32	119.22	119.20
C20	C18	C16	121.72(17)	121.44	121.47	121.35	121.40
C18	C20	C12	119.07(16)	119.24	119.08	119.37	119.48

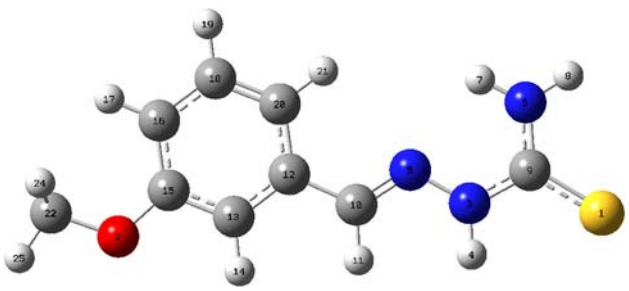

Figure 1. CAM-B3LYP optimized geometry of **I** with atomic labeling.

are 100–500 cm^{-1} apart from the experimental result. This deviation is because of the negligence of anharmonic effect as well as the difference in the phase of the compound [experiment (solid) and computation (gas)]. The calculated wave numbers are multiplied with appropriate scale factor which is derived empirically for better matching with the experimental value. Scaling of frequencies brings them much closer to the experimentally obtained frequencies. Electron distribution in the frontier molecular orbital (HOMO and LUMO) is shown in Figure 2 which indicates that the HOMO is centered on the sulphur and nitrogen atom and LUMO is localized over the benzene ring. The calculated HOMO and LUMO orbital energy, energy gap, hardness, softness and dipole moment values are presented in Table 3. The binding ability of a ligand with a metal is

Table 3. HOMO and LUMO energies, HOMO–LUMO energy gap, hardness (η) in eV, softness (σ) in eV^{-1} and dipole moment (μ) values in Debye of compound **I**.

HOMO	LUMO	E_{gap}	η	σ	μ
−5.9326	−1.9891	3.9435	−1.9718	0.5072	6.9354

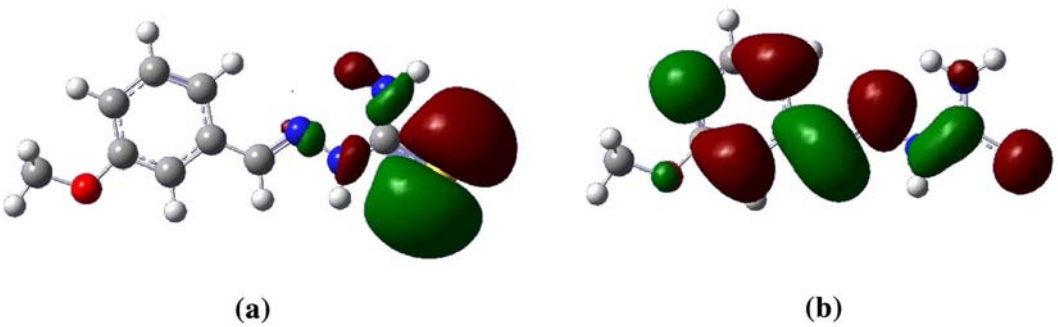

Figure 2. Calculated (a) HOMO and (b) LUMO of **I** at CAM-B3LYP method.

Table 4. Atomic charges derived from electrostatic potential (a.u.) calculated by CHELPG scheme at various computational method using 6-311++G(d,p) basis set of **I.** [* for MP2 the basis set is 6-311+G(d)].

Sl. No.	Atom	CAM/B3LYP	MP2	HF
1	S	−0.446999	−0.524461	−0.529258
2	O	−0.420263	−0.448394	−0.441819
3	N	0.051512	−0.256403	0.016352
4	H	0.141562	0.231229	0.154084
5	N	−0.272584	−0.230714	−0.301031
6	N	−0.545494	−0.724537	−0.571859
7	H	0.299256	0.366565	0.317284
8	H	0.311220	0.340669	0.317871
9	C	0.241996	0.527073	0.320199
10	C	−0.003574	0.094801	0.056001
11	H	0.151627	0.153405	0.160823
12	C	0.240241	0.155944	0.244773
13	C	−0.415153	−0.414201	−0.456642
14	H	0.134153	0.153699	0.152112
15	C	0.536938	0.549474	0.567139
16	C	−0.341990	−0.366801	−0.353781
17	H	0.155319	0.172286	0.161398
18	C	−0.018720	−0.022032	−0.018524
19	H	0.100654	0.117540	0.116118
20	C	−0.235445	−0.223844	−0.279726
21	H	0.106412	0.105252	0.128134
22	C	0.148045	0.163977	0.164845
23	H	0.011607	0.008537	0.010344
24	H	0.011712	0.013539	0.010382
25	H	0.057966	0.057397	0.054782

directly proportional to the HOMO energy. Further the HOMO–LUMO energy gap is a measure of the stability of a compound. The hardness and softness are important parameters in understanding chemical reactivity and stability. Smaller the value of hardness higher is the reactivity of a compound. The dipole moment is another parameter which is used as stability index of a ligand. A ligand with higher dipole moment values produces more stable compounds. These data will definitely help in understanding of the reactivity of the compound **I** with transition metals. The partial atomic charge describes the electron charge distribution within molecule and is a useful descriptor in understanding donor and acceptor ability of an atom in a molecule. The partial atomic charges calculated by CHELPG scheme at different computational methods are presented in Table 4. It can be observed that results obtained in different computational methods do not vary significantly and are very close to each other except few cases indicating the efficiency of CHELPG scheme. The data shows that all the hydrogen atoms have net positive charge. The presence of large negative charge on S and N atom suggests the formation of intermolecular interaction with H atoms. This result commensurates with the results obtained from the solid crystalline structure with the formation of hydrogen bonds.

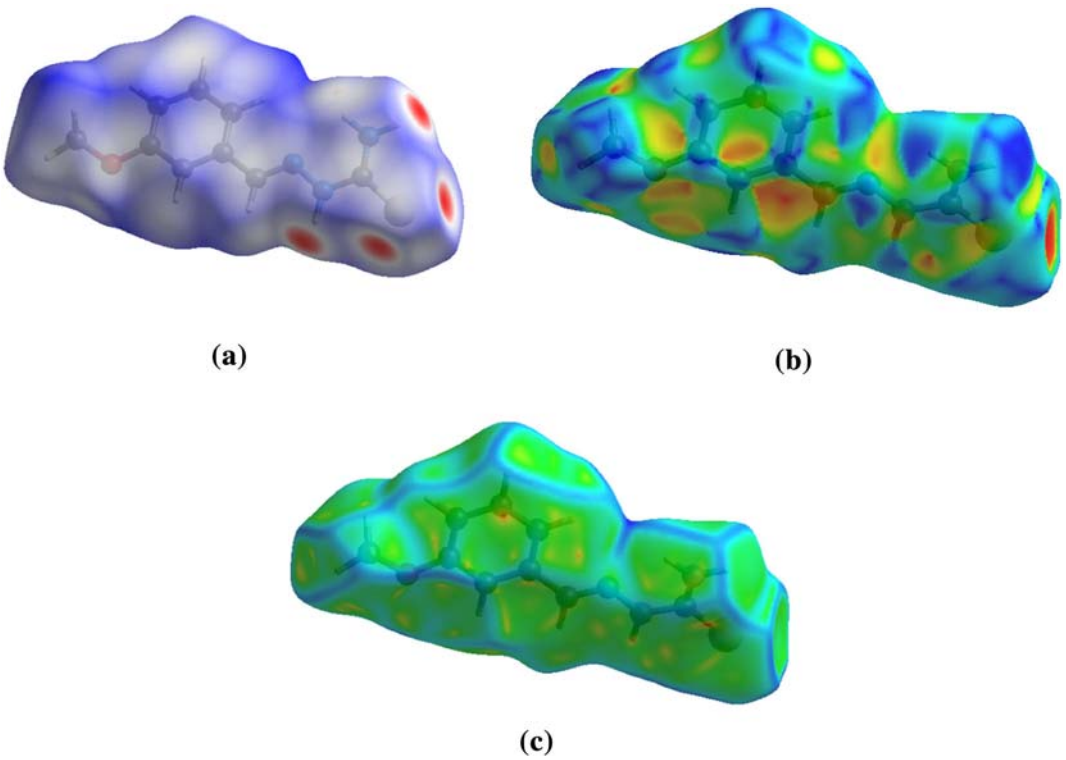

Figure 3. Hirshfeld surfaces mapped for (a) d_{norm} surfaces, (b) shape index and (c) curvature of 3-anisaldehyde thiosemicarbazone.

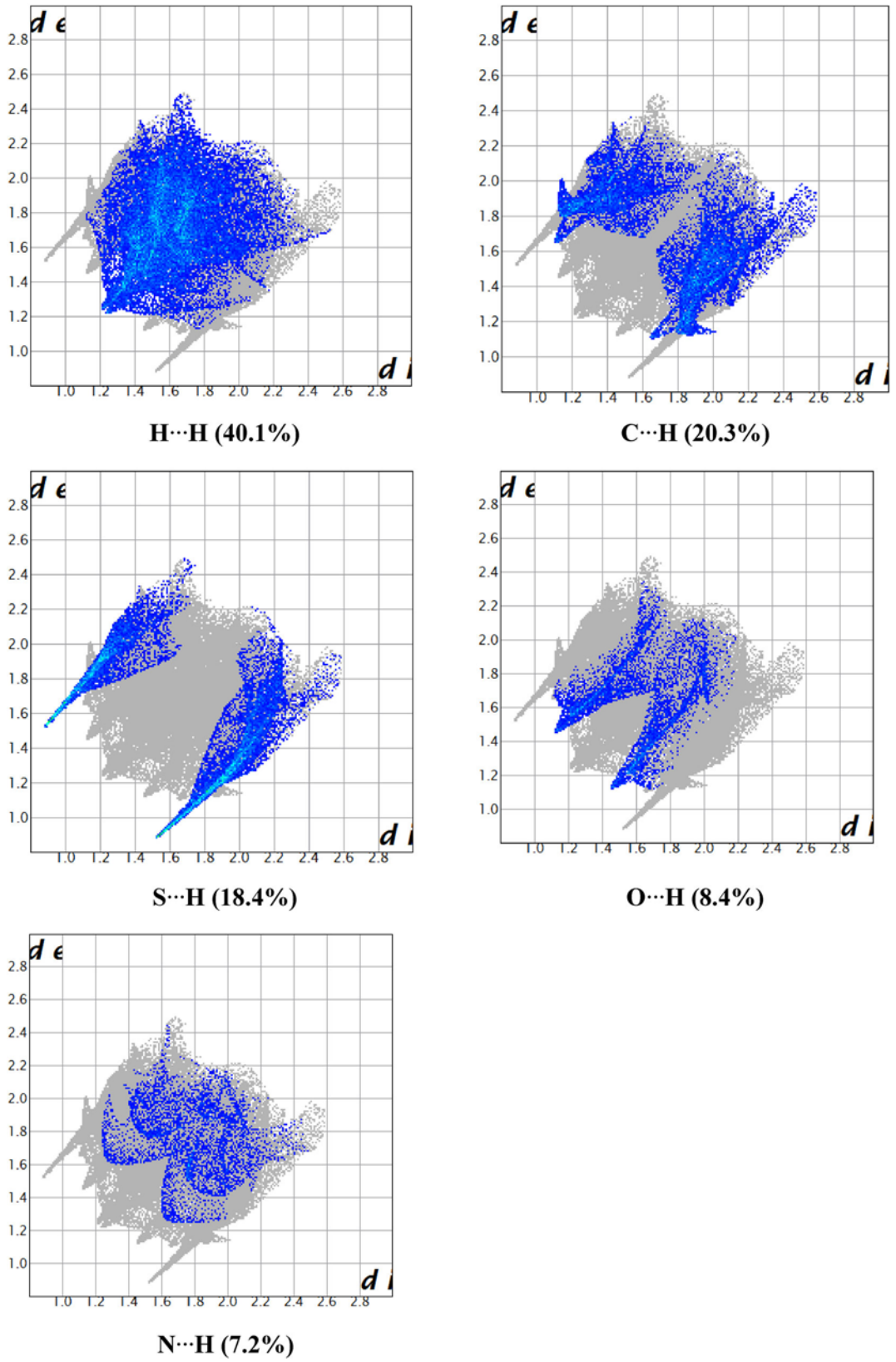

Figure 4. Relative contributions to the percentage of Hirshfeld surface area for the various intermolecular contacts in compound **I**.

3.3 *Hirshfeld surface studies*

Molecular Hirshfield surfaces comprising of *d*norm surface, shape index and curvedness of compound **I** were generated using a standard (high) surface resolution and is illustrated in Figure 3. The d_{norm} surface was mapped on over the range of −0.3276 a.u. to +1.2461a.u, shape index in the range of −0.9976 a.u. to 0.9988 a.u. and curvature in the range of −3.5221 a.u. to 0.4621 a.u. The d_{norm} mapping indicates strong N-H···S hydrogen bonding interaction as primary interaction seen as bright red spot. The two dimensional (2D) fingerprint plots from Hirshfeld surface analyses of the title compound are shown in Figure 4 which illustrate the relative contribution (in percentage) of the major intermolecular contacts associated with it. The 2D Finger print plots complement the Hirshfeld surface by summarizing the nature and type of intermolecular contacts in a quantitative manner. The most important interaction is H···H with contribution of 40.1% to the overall crystal packing. Further, the S···H (18.4%), C···H (20.3%), N···H (7.2%) and O···H (8.4%) FP plots also reveal the information regarding the intermolecular hydrogen bonds with individual contribution towards crystal packing. N-H interaction (indicated by two large spikes) is one of the most significant contacts. The FP plot of C-H contacts shows characteristics "wings" which are identified as a result of weak C-H···π interactions. The red triangles on the shape index represented by concave regions indicate π-stacking interactions whereas the blue triangles represented by convex regions indicate the ring atoms of the molecule inside the surface. The red triangles on the shape index mapping refer to the C-H···π interaction with the contribution of 20.3% which is in accordance with the 2D FP plot. The curvedness indicates the electron density of surface curves around the molecular interactions. The flat areas of the surface correspond to low value of curvedness, while sharp curvature area corresponds to high values of curvedness and usually tends to divide the surface into patches, indicating contacts between neighbouring molecules. The large flat region delineated by a blue outline refers to π-π stacking interactions. Curvedness of the present compound indicates absence of π-π stacking interactions.

3.4 *Molecular docking study*

The best binding mode of docked compound **I** with Human Topoisomerase III beta domain (5GVC) and Human thioredoxin reductase-thioredoxin complex (3QFA) is shown in Figure 5 and Figure 6 respectively. Further the docking interaction with **II** has been depicted in Figure S6 and Figure S7 respectively. The analysis from the molecular docking study helps to find out various types of interactions like H-bonding, hydrophobic and electrostatic interactions. The docking results are reported in Table 5. The compound **I** was extended into the active site of 5GVC with amino acid residues TRP 73, LYS 72, ARG 194, ASP 74, GLN 201, LYS 198, LYS 75, PRO 78 and VAL 76. The binding mode of this enzyme with the compound exhibited two hydrogen bonds with amino acid residues GLN 201 and VAL 76. This interaction reveals a favourable binding energy, attractive and repulsive van der waals energy. The same compound

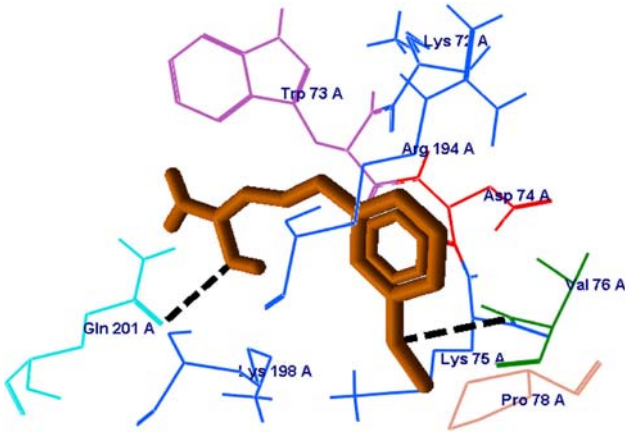

Figure 5. Docking Interaction of amino acid residues of enzyme 5GVC (green and light blue colors) with **I** (brown color). One acidic amino acid (aspartic acid) and the other polar amino acid (glutamine) is involved in hydrogen bonding with the ligand (black dotted line).

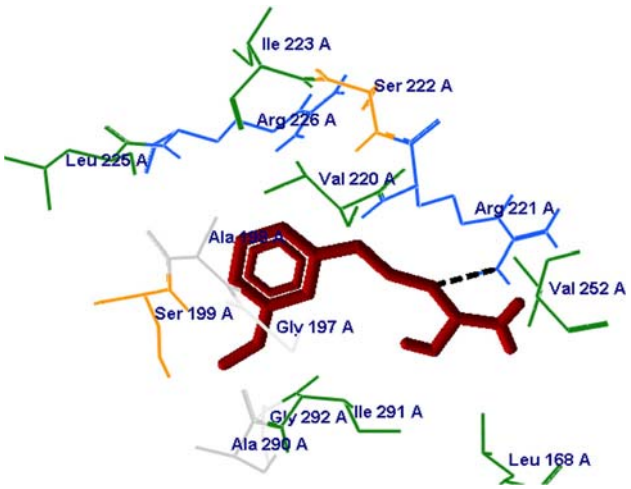

Figure 6. Docking Interaction of an amino acid residues of enzyme, 3QFA (light blue)with ligand, **I** (maroon). Only one basic amino acid (arginine) is involved in hydrogen bonding.

Table 5. Molecular docking results of 2-anisaldehyde thiosemicarbazone (**II**) and 3- anisaldehyde thiosemicarbazone (**I**) with 5GVC and 3QFA.

Compound (C)	Enzyme (E)	Amino acid (A.A)	Type of hydrogen bond interaction (L···A.A of E)	Binding fee energy (Kcal/mole)	Bond length (A^0)
II	5GVC	Asp 511	S···H-O	−32.81	3.145
		Asp 386	N···H-O or N-H···O=C		2.883
I	5 GVC	Gln201	S-H···O=C Or S···H-O	−33.89	3.017
		Val76	O···H-N		3.493
II	3 QFA	Arg 100	S-H···O=C Or S…H-O	−32.39	3.447
		Glu 103	S-H···O-H Or S···H-O		2.674
I	3 QFA	Arg221	N-H···N-H	−29.93	3.335

was then docked into the active site of 3QFA with amino acid residues ILE223, SER222, ARG 221, LEU 225, VAL 220, ARG 221, VAL 252, ALA198, SER199, GLY 197, GLY 292, ILE 291, ALA 290 and LEU 168. The results indicated the interaction of the compound with the enzyme's active site creating one hydrogen bond with ARG 221. Table 5 also depicts the results of the binding interaction of **II** with 5GVC and 3QFA enzymes. The interaction of **II** with 3QFA results in the formation of two hydrogen bonds with ARG 100 and GLU 103 and the interaction with 5GVC shows two hydrogen bonds with ASP 511 and ASP 386. Various types of hydrogen bond interactions (N-H•••O, N-H···N, O-H···N, S-H···N, SH···O, S···H-O, S···H-N) have been exhibited during the interaction. Binding energy of **I** with 5GVC and 3QFA was found to be −33.89 Kcal/mole and −29.93 Kcal/mole respectively whereas in the case of **II** it was −32.81 Kcal/mole and −32.39 Kcal/mole respectively. The molecular docking analysis suggests that **I** binds stronger than **II** with 5GVC with a binding free energy difference of 1.08 kcal/mol and also with 3 QFA with an attractive van der Waals difference of 1.03 kcal/mol (provided as PDB docking files as supplement). The better binding ability of **I** can be explained from the structural difference between compound **I** and **II** in terms of change in the position of methoxy group. The methoxy group at ortho position provides steric hindrance which is much lesser in meta position. The evidence of steric effect at ortho position interrupting the optimum interaction of the ligand with the enzyme has been reported.[30, 31] On account of the electron donating nature of methoxy group in an aromatic ring, the ortho and para positions get activated. Thus activity at ortho- and para-substituted compounds are higher compared to meta-substituted compound. The inhibitory potency of meta-substituted compounds is generally higher than their ortho- and para-substituted analogues.

4. Conclusion

The heterocyclic N-S donor ligand, 3-anisaldehyde thiosemicarbazone, can be modeled theoretically using DFT methods at CAM-B3LYP level. Molecular Hirshfeld surface analysis revealed the primary interaction to be H···H, C···H, and S···H interaction to govern the solid state packing and the 2D finger print plots quantitatively map out these interactions. The results indicate that this compound can be employed for designing of related supramolecular systems. The docking studies reveal that the studied compound can be a suitable and potential drug candidate for the enzyme Human topoisomerase III beta domain. There is considerable change in binding affinity with change in the position of methoxy group from meta to ortho. By modulating the effect of methoxy substituent on phenyl ring, the bonding behaviour of thiosemicarbazone compounds can be altered. These studies can also be extended to examine their effect on various in vitro investigations of microbiological and cytotoxic properties.

5. Supplementary material

CCDC 1553591 contains the supplementary crystallographic data for 3-anisaldehyde thiosemicarbazone. These data can be obtained free of charge from Cambridge Crystallographic Data Centre viawww.ccdc.cam.ac.uk/data_request/cif or from the Cambridge Crystallographic Data Centre, 12 Union Road,

Cambridge CB2 1EZ, UK; Fax: (+44) 123-336-033 or E-mail:deposit@ccdc.cam.ac.uk.

Top ten results as PDB docking files mentioning various energies and other relevant information are also provided.

Crystallographic information and quantum chemical calculations (optimized coordinates and IR vibrational frequencies) are given in supporting information.

Acknowledgement

The authors are greatly indebted to Prof. Jerry P. Jasinski, Keene State College, for X-ray crystallography, Prof. Rajiv Gupta, Delhi University for providing NMR spectra. The authors also thank Sharda University for providing computing facility. BE gratefully acknowledges research grant from Science and Engineering Research Board through Young Scientist Scheme (Grant no.YSS/2015/000685). Finally the authors are grateful to the reviewer for the suggestions which have been helpful in improving the quality of this manuscript.

Compliance with ethical standards

Conflict of interest The authors declare no conflicts of interest.

References

1. Lobana T S, Sharma R, Bawa G and Khanna S 2009 Bonding and structure trends of thiosemicarbazone derivatives of metals—an overview *Coord. Chem. Rev.* **253** 977
2. Lobana T S, Indoria S, Jassal A K, Kaur H, Arora D S and Jasinski J P 2014 Synthesis, structures, spectroscopy and antimicrobial properties of complexes of copper(II) with salicylaldehyde N- substituted thiosemicarbazones and 2,2'-bipyridine or 1,10-phenanthroline *Eur. J. Med. Chem.* **76** 154
3. West D X, Liberta A E, Padhye S B, Chikate R C, Sonawane P B, Kumbhar A S and Yerande R G 1993 Thiosemicarbazone complexes of copper(II): structural and biological studies *Coord. Chem. Rev.* 123 49
4. Mahajan R K, Kaur I and Lobana T S 2003 A mercury (II) ion-selective electrode based on neutral salicylaldehyde thiosemicarbazone *Talanta* **59** 101
5. Ali M A, Khalifa M E, Ghazy S E and Hassanien M M 2002 Selective flotation-separation and spectrophotometric determination of cadmium using phenanthraquinone monophenythiosemicarbazone *Anal. Sci.* **18** 1235
6. Malarz K, Mrozek-Wilczkiewicz A, Serda M, Rejmund M, Polanski J and Musiol R 2018 The role of oxidative stress in activity of anticancer thiosemicarbazones *Oncotarget* **9** 17689
7. Serda M, Kalinowski D S, Rasko N, Potuckova E, Mrozek-Wilczkiewicz A, Musiol R, Malecki J G, Sajewicz M, Ratuszna A, Muchowicz A, Golab J, Simunek T, Richardson D R and Polanski J 2014 Exploring the anti-cancer activity of novel thiosemicarbazones generated through the combination of retrofragments: dissection of critical structure-activity relationships *Plos One* **9** 110291
8. Eckhardt S 2002 Recent progress in the development of anticancer agents *Curr. Med. Chem. Anti-cancer Agents* **2** 419
9. Siegel R, Naishadham D and Jemal A 2012 Cancer statistics *CA Cancer J. Clin*. **62** 10
10. Kalinowski D S, Quach P and Richardson D R 2009 Thiosemicarbazones: The new wave in cancer treatment *Future Med. Chem.* **1** 1143
11. Arora S K, Agarwal S and Singhal S 2014 Anticancer activities of thio semicarbazides/thiosemicarbazones *Int. J. Pharm. Pharm. Sci.* **6** 34
12. Molinari A Oliva A, Ojeda C, Miguel J M, Castro M A, Cuevas C and Feliciano A S 2008 Synthesis and cytotoxic evaluation of 6-(3-pyrazolylpropyl) derivatives 1,4-naphthohydroquinone-1,4-diacetate *Arch. Pharm. Chem. Life Sci.* **341** 301
13. Kongkathip N, Kongkathip B, Siripong P, Sangma C, Luangkamin S, Niyomdecha M, Pattanapa S, Piyaviriyagul S and Kongsaeree P 2003 Potent antitumor activity of synthetic 1,2-Naphthoquinones and 1,4-Naphthoquinones *Bioorg. Med. Chem.* **11** 3179
14. David R da Rocha, Ana C G de Souza, Jackson A L C Resende, Wilson C Santos, Evelyne A dos Santos, CláudiaPessoa, Manoel O. de Moraes, Letícia V. Costa-Lotufo, Raquel C Montenegro and Vitor F Ferreira 2011 Synthesis of new 9-hydroxy-α- and 7-hydroxy-β-pyran naphthoquinones and cytotoxicity against cancer cell lines *Org. Biomol. Chem.* **9** 4315
15. McClendon A K and Osheroff N 2007 DNA Topoisomerase II, genotoxicity, and cancer *Mutat. Res.* **623** 83
16. Lu J, Chew E H and Holmgren A 2007 Targeting thioredoxin reductase is a basis for cancer therapy by arsenic trioxide *Proc. Natl Acad. Sci*. **104** 12288
17. Zhang J, Wu L-P, Zhuang L-H and Wang G-W 2009 3-Methoxybenzaldehyde thiosemicarbazone *Acta Cryst.* ***E65*** o884
18. Gaussian 16, Revision C.01, Frisch M J, Trucks, G W, Schlegel H B, Scuseria, G E, Robb M A, Cheeseman J R, Scalmani G, Barone V, Petersson G A, Nakatsuji, H, Li X, Caricato M, Marenich A V, Bloino J, Janesko B G, Gomperts R, Mennucci B, Hratchian H P, Ortiz J V, Izmaylov A F, Sonnenberg J L, Williams-Young D, Ding F, Lipparini F, Egidi F, Goings J, Peng B, Petrone A, Henderson T, Ranasinghe D, Zakrzewski V G, Gao J, Rega N, Zheng G, Liang W, Hada M, Ehara M, Toyota K, Fukuda R, Hasegawa J, Ishida M, Nakajima T, Honda Y, Kitao O, Nakai H, Vreven T, Throssell K, Montgomery J A, Jr. Peralta J E, Ogliaro F, Bearpark M J, Heyd J J, Brothers E N, Kudin K N, Staroverov V N, Keith T A, Kobayashi R, Normand J, Raghavachari K, Rendell A P, Burant J C, Iyengar S S, Tomasi J, Cossi M, Millam J M, Klene M, Adamo C, Cammi R, Ochterski J W, Martin R L, Morokuma K, Farkas O, Foresman J B and Fox D J, Gaussian Inc. Wallingford CT, 2016.
19. Yanai T, Tew D P and Handy N C 2004 A new hybrid exchange-correlation functional using the Coulomb-

attenuating method (CAM-B3LYP) *Chem. Phy. Lett.* **393** 51
20. Pearson R J 1985 Absolute electronegativity and absolute hardness of Lewis acids and bases *J. Am. Chem. Soc.* **24** 6801
21. Breneman C M and Wiberg K B 1990 Determining atom-centered monopoles from molecular electrostatic potentials – the need for high sampling density in formamide conformational-analysis *J. Comp. Chem.* **11** 361
22. Turner M J, McKinnon J J, Wolff S K, Grimwood D J, Spackman P R, Jayatilaka D and Spackman M A 2017 *CrystalExplorer17*. The University of Western Australia.
23. Spackman M A and Dylan J 2009 Hirshfeld surface analysis *CrystEngComm.* **11** 19
24. Seth S K, Saha N C, Ghosh S and T Kar 2011 Structural elucidation and electronic properties of two pyrazole derivatives: A combined X-ray, Hirshfeld surface analyses and quantum mechanical study *Chem. Phys. Lett.* **506** 309
25. Venkatesan P, Thamotharan S, Ilangovan A, Liang H and Sundias T 2016 Crystal structure, Hirshfeld surfaces and DFT computation of NLO active (2E)-2-(ethoxycarbonyl)-3-[(1-methoxy-1-oxo-3-phenylpropan-2-yl) amino] prop-2-enoic acid *Spectrochim. Acta Part A* **153** 625
26. Dina S-D, Yuval I, Ruth N and Haim J W 2005 PatchDock and SymmDock: servers for rigid and symmetric docking *Nucleic Acids Res.* **33(2)** 363
27. Haque R A and Salam M A 2015 Synthesis, structural, and spectral studies of diorganotin(IV) complexes with 2–hydroxy-5-methylbenzaldehyde-*N*(4)-cyclohexylthiosemicarbazone *J. Coord. Chem.* **6** 714
28. Mbah J A, Ayimele G A, Kodjiyo N, Yong J N, Nfor E N and Gatsing D 2017 Synthesis, molecular structure and antibacterial activity of 1-(4-methoxybenzaldehyde)-4-Methyl-thiosemicarbazone *Int. J. Org. Chem.* **7** 229
29. Oliveira A B, Feitosa B R S, Näther C and Jess I 2014 Bis(4-hydroxy-3-methoxy-benzaldehyde 4-phenyl-thiosemicarbazonato-N^1,S) nickel(II) *Acta Cryst.* **E70** m195
30. Bahmani Y, Bahrami T and Aliabadi A 2019 Synthesis, cytotoxicity assessment and molecular docking of N-(5-(substituted-benzylthio)-1,3,4-thiadiazole-2-yl)-2-p-fluorophenylacetamide derivatives as tyrosine kinase inhibitors *Indian J. Pharm. Sci.* **81** 70
31. Samad A, Naffaa M M, Bakht M A, Malhotra M and Ganaie M A 2014 Target based designing of anthracenone derivatives as tubulin polymerization inhibiting agents: 3D QSAR and docking approach *Int. J. Med. Chem.* **2014** 658016